Photosynthesis Research (2023) 158:171–180
https://doi.org/10.1007/s11120-023-01044-8

RESEARCH

Revealing the significance of chlorophyll *b* in the moss *Physcomitrium patens* by knocking out two functional chlorophyllide *a* oxygenase

Lin Zhang[1,2,3] · Chunhong Yang[1,2] · Cheng Liu[1,2]

Received: 18 May 2023 / Accepted: 11 August 2023 / Published online: 31 August 2023

Abstract

The chlorophyllide *a* oxygenase (CAO) plays a crucial role in the biosynthesis of chlorophyll *b* (Chl *b*). In the moss *Physcomitrium patens* (*P. patens*), two distinct gene copies, *PpCAO1* and *PpCAO2*, are present. In this study, we investigate the differential expression of these CAOs following light exposure after a period of darkness (24 h) and demonstrate that the accumulation of Chl *b* is only abolished when both genes are knocked out. In the *ppcao1cao2* mutant, most of the antenna proteins associated with both photosystems (PS) I and II are absent. Despite of the existence of LHCSR proteins and zeaxanthin, the mutant exhibits minimal non-photochemical quenching (NPQ) capacity. Nevertheless, the *ppcao1cao2* mutant retains a certain level of pseudo-cyclic electron transport to provide photoprotection for PSI. These findings shed light on the dual dependency of Chl *b* synthesis on two CAOs and highlight the distinct effects of Chl *b* deprival on PSI and PSII core complexes in *P. patens*, a model species for bryophytes.

Keywords *Physcomitrium patens* · Chlorophyll *b* · Chlorophyllide *a* oxygenase · Light harvesting complexes (LHC)

Introduction

Oxygenic photosynthesis sustains most life on earth by converting light to chemical energy. Plants evolved various light harvesting complexes (LHCs) to capture sunlight under different conditions. However, excess light can cause photodamage to the photosynthetic apparatus (Perrine et al. 2012; Friedland et al. 2019; Wu et al. 2020). To prevent this, plants employ a rapid photoprotective mechanism called nonphotochemical quenching (NPQ) that dissipates excess energy as heat mostly in LHCs (Müller et al. 2001; Derks et al. 2015; Giovagnetti and Ruban 2018). The moss *Physcomitrium patens* (*P. patens*) has a diverse LHC system that includes both algal- and angiosperm-type NPQ pathways, unlike the green alga *Chlamydomonas reinhardtii* (*Chlamydomonas*) and the flowering plant *Arabidopsis thaliana* (*Arabidopsis*) that have one type each. (Gerotto et al. 2012; Ilik et al. 2017).

Chlorophyll (Chl) *b* only exists in the LHCs and play critical roles in stabilizing them (Green and Durnford 1996; Horn et al. 2007; Tanaka and Tanaka 2011). Chl *b* is synthesized from Chl *a* by the action of chlorophyllide a oxygenase (CAO), a key enzyme with three domains: A (regulatory), B (linker), and C (catalytic) (Oster et al. 2000; Eggink et al. 2004; Nagata et al. 2004; Kunugi et al. 2013). CAO is usually encoded by a single gene in green plants, except for rice which also has a pseudogene (Tanaka et al. 1998; Nagata et al. 2004; Lee et al. 2005; Kunugi et al. 2013; Bujaldon et al. 2017; Jung et al. 2021). In the prasinophyte *Micromonas*, the Rieske center and mononuclear iron-binding motif of the conserved site in C domain of CAO is encoded by different genes (Kunugi et al. 2013). The *CAO* knockout in *Chlamydomonas* and *Arabidopsis* leads to the absence of Chl *b* and the reduction of LHCs, especially LHCII. However, some PSII dimer and PSI-LHCI complex remain on the thylakoid membranes of these mutants (Tanaka and Tanaka 2005; Havaux et al. 2007; Kim et al. 2009; Dall'Osto et al. 2010; Takabayashi et al. 2011; Bujaldon et al. 2017). In the genome of *P. patens*, two complete *CAO* genes (*PpCAO1* and *PpCAO2*) were detected in two chromosomes (Rensing et al. 2008), with unidentified physiological significance.

✉ Cheng Liu
liucheng@ibcas.ac.cn

[1] Photosynthesis Research Center, Key Laboratory of Photobiology, Institute of Botany, Chinese Academy of Sciences, Beijing 100093, China

[2] University of Chinese Academy of Sciences, Beijing 100049, China

[3] Institute of Biotechnology, Beijing Academy of Agriculture and Forestry Sciences, Beijing, China

In this study, we employed CRISPR-Cas9 technology to knock out both CAO genes, thereby generating a Chl *b*-less mutant of *P. patens*, namely *ppcao1cao2*. We showed that both CAOs were essential for Chl *b* synthesis in the moss. Notably, the loss of Chl *b* had a more pronounced impact on the PSII core complexes compared to the PSI core complexes. This discrepancy may be attributed to the diminished NPQ observed in *ppcao1cao2*, which serves as the primary photoprotective mechanism for PSII. Nonetheless, the mutant displayed evident pseudo-cyclic electron transport, which acts as a safe valve for the acceptor side of PSI.

Experimental procedures

Plant culture, transformation and treatments

Plants were cultivated in a growth chamber under controlled conditions, including a 16 h light: 8 h dark photoperiod, 60% humidity, 23 °C and 50 µmol photons m^{-2} s^{-1} light intensity. *P. patens* Gransden wild-type strain was grown on solidified minimum $PpNO_3$ medium supplemented with 0.5% glucose (Ashton et al. 1979; Pinnola et al. 2013, 2015, 2018; Yan et al. 2021). To disrupt the *PpCAO1* and *PpCAO2* genes, three target sites (Table S1) were selected for designing sgRNA (single-guide RNA) using the webtool CRISPR V1 against *P. patens* genome Phytozome V9 (http://crispor.tefor.net/crispor.py). CRISPR/Cas9 constructs were generated following a previously established protocol (Lopez-Obando et al. 2016). Protoplast isolation and transformation were performed using two rounds of 5-day-old moss protonema tissues (Ashton et al. 1979; Schaefer and Zrÿd 1997; Lopez-Obando et al. 2016). Subsequently, genome sequencing confirmed the generation of *ppcao1*, *ppcao2*, and *ppcao1cao2* mutants.

Thylakoid extraction and gel electrophoresis

Thylakoid membranes were extracted from 10-day-old protonema tissues as described (Gerotto et al. 2012, 2019). Two different techniques, denaturing SDS-PAGE and lpBN-PAGE followed by 2D SDS-PAGE, were employed. For denaturing SDS-PAGE, thylakoids were solubilized with Laemmli buffer and separated by SDS-PAGE. Proteins were stained with Coomassie brilliant blue G250 or transferred to polyvinyl difluoride membranes and immunoblotted with the corresponding antibodies (the D1 (AS05084), D2 (AS06146), CP47 (AS04038), CP43 (AS06110), PSBS (AS09533), PSAB (AS10695), LHCA2 (AS01006), ATP β subunit (AS08370), Cyt b_6 (AS03034) and Cyt *f* (AS06119) were purchased from Agrisera and the LHCBM, LHCSR, LHCB5 and LHCB6 were synthesized by Thermo-Fisher Co. For lpBN-PAGE followed by 2D SDS-PAGE, thylakoid membranes were first solubilized with 1% (w/v) β-DM at a final Chl concentration of 0.5 µg/µL and separated by lpBN gel system (Järvi et al. 2011). Then lanes were cut and solubilized with Laemmli buffer and separated by SDS-PAGE. Finally, the proteins were visualized by either CBB staining or western blotting.

Low-temperature fluorescence emission spectra

The thylakoid membranes were extracted and then rapidly frozen in liquid nitrogen at 20 µg/mL chlorophyll concentration (Casazza et al. 2001). The low temperature fluorescence emission spectra measurements were performed by exciting at 475 nm and recording in the 600–800 nm range. There were three major peaks: 682, 693 and 717 nm, which were attributed to LHCII, PSII core and PSI-LHCI respectively (Pinnola et al. 2015).

In vivo measurements of chlorophyll fluorescence

In vivo chlorophyll fluorescence was monitored with a Dual-PAM-100 (Walz, Germany). Plants were dark-acclimated for 30 min before measurements. The NPQ kinetics using 830 µmol photons m^{-2} s^{-1} of actinic light was measured for 10 min with saturating light of 6000 µmol photons m^{-2} s^{-1} and then for 10 min in dark.

Estimation of the functional antenna size of PSII and PSI

The relative antenna size of PSI was estimated according to the method described previously (Iwai et al. 2015; Pinnola et al. 2015) by analyzing time courses of P700 photooxidation upon illumination of the protonema with far-red light (710 nm, 200 µmol photons m^{-2} s^{-1}). The kinetics were measured using a LED excitation-detection spectrometer JTS-10 (Bio-logic, France), and the protonema incubated with 30 µM DCMU and 100 µM MV in the dark for 40 min.

The relative antenna size of PSII was estimated by measuring the induction of Chl fluorescence emitted by *P. patens* protonema infiltrated with 20 µM DCMU for 30 min as described previously (Malkin et al. 1981; Havaux et al. 2007). The Chl fluorescence kinetics were measured using a Plant Efficiency Analyser (Hansatech, UK).

High-performance liquid chromatography

The chlorophyll concentrations were determined following extraction of the pigments in acetone as described previously (Yang et al. 1999) and the pigment compositions were analyzed by HPLC as described (Thayer and Björkman 1990; Qin et al. 2015). Briefly, 0.1 g fresh green tissues were used for extraction in a certain amount of acetone and the final

volume and the pigment concentration after each extraction were measured. Each sample of 0.12 µg Chl amount was injected in the HPLC instrument to fit in the quantitative range. The pigment compositions were calculated based on the fresh weight of green tissues.

qRT-PCR

The transcripts were quantified by qRT-PCR using specific primers listed in Table S3. For qRT-PCR analysis, the first strand of cDNA was synthesized from total RNA prepared from 10 day-old protonemata, and qRT-PCR was performed using 2 × HQ SYBR qPCR Mix (High ROX) (ZOMANBIO) with the following thermal cycling program: 95 °C for 30 s, followed by 40 cycles of 95 °C for 10 s, 60 °C for 30 s. The data were analyzed using LightCycler480 Software release 1.5.0 (Roche). The relative gene expression levels were normalized by the Actin gene. qRT-PCR was carried out in duplicate for each sample in three independent experiments.

Statistical analysis

All experiments were repeated at least three times ($n \geq 3$). Values are expressed as mean ± SD. One-way ANOVA and Tukey's multiple comparison test were used to determine the significant difference between different treatments ($\alpha = 0.05$).

Results

The transcriptional level of two *CAO* genes

Two *CAO* homologous genes, *PpCAO1* and *PpCAO2* (Pp3c19_22390 and Pp3c22_20970 in *P. patens* genome v3.3: https://phytozome-next.jgi.doe.gov/), in *P. patens* are detected on chromosome 19 and 22 respectively with 80% homology. Motif analysis shows that both *CAO* genes possess the characteristic domains found in *CAO* genes of other species (Figs. S1–2). Phylogenetic analysis shows that the *CAO* genes of *P. patens* a occupy an intermediate position between those of green algae and vascular plants, but exhibit closer evolutionary affinity to the latter group (Fig. S3). Expression analysis revealed that both *PpCAO1* and *PpCAO2* are transcribed under both dark and light conditions (Fig. S4), which differs from the expression pattern observed in rice CAOs (Lee et al. 2005). To investigate the temporal expression profiles, quantitative real-time PCR (qRT-PCR) was performed at different time points (0.5, 1, 2, 4, 6, and 240 h) after 24 h of darkness followed by illumination. The results indicated that the expression level of *PpCAO1* remains relatively constant regardless of the duration of light exposure. In contrast, the expression of *PpCAO2* closely resembles that of *PpCAO1* up to 4 h of light treatment, but shows significant upregulation thereafter (Fig. 1).

The *ppcao1cao2* mutant possesses very low PS activities

We employed the CRISPR-Cas9 technology to simultaneously knock out *PpCAO1* and *PpCAO2* genes in order to investigate the consequences of Chl *b* deprivation. The *ppcao1*, *ppcao2, ppcao1cao2* mutants were identified by sequencing (Fig. S5). Analysis of pigment composition revealed a significant reduction in Chl *b* level in *ppcao1* and *ppcao2* than in WT (Fig. S6) Intriguingly, Chl *b* was completely absent in *ppcao1cao2*, which also exhibited approximately half the Chl *a* concentration of WT. Meanwhile, *ppcao1cao2* displayed a distinct paler phenotype, accompanied by a substantial decrease in xanthophyll pigments. Importantly, the mutant exhibited a very low Fv/Fm, the maximum quantum yield of PSII, measuring only approximately about two-third of observed in the WT, indicating that strong PSII photoinhibition existed in *ppcao1cao2* (Table 1, Fig. S7).

The induction of Chl *a* fluorescence with the presence of DCMU and P700 photoreduction with the presence of DCMU and MV were measured to reflect the estimated the functional antenna size for PSII and PSI (Malkin et al. 1981; Greene et al. 1988; Iwai et al. 2015; Pinnola et al. 2015; Bujaldon et al. 2017). The functional antenna size of both PSs was severely reduced in *ppcao1cao2* compared with WT (Fig. 2a, b).

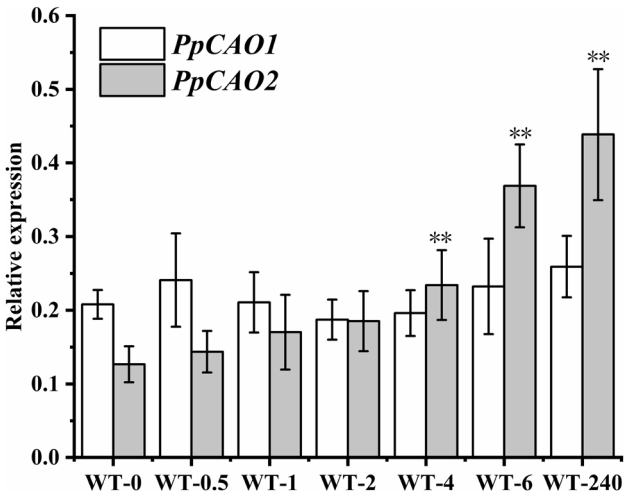

Fig. 1 The expression levels of *PpCAO1* and *PpCAO2* in *P. patens* WT under grown light. WT-0 ~ WT-240, the time of light treatment. Significant differences according to Tukey's multiple comparison test ($\alpha < 0.05$) are marked with the asterisks. All data are expressed as mean ± SD ($n \geq 3$)

Table 1 The pigment stoicheiometry of WT and the *cao* double mutant of *Physcomitrium patens* under growing light for 5d

Pigments composition (μg/g FW)	Neo	Vio	Lut	Zea	Chl *b*	Chl *a*	B-Car	Fv/Fm
WT	15.97 ± 0.69^{a}	22.04 ± 1.51^{a}	34.96 ± 0.70^{a}	9.71 ± 1.38^{a}	167.69 ± 3.90^{a}	428.93 ± 12.8^{a}	9.39 ± 0.73^{a}	0.77 ± 0.03^{a}
ppcao1cao2	3.48 ± 0.14^{b}	11.37 ± 0.94^{b}	13.66 ± 0.46^{b}	3.82 ± 0.40^{b}	nd	198.55 ± 7.34^{b}	7.47 ± 0.56^{ab}	0.52 ± 0.11^{b}

Neo Neoxanthin, *Vio* Violaxanthin, *Lut* Lutein, *Zea* Zeaxanthin, Chl *b* Chlorophyll *b*, Chl *a* Chlorophyll *a*, *β*-Car Beta carotene, *Fv/Fm* the maximum quantum yield of PSII, *FW* fresh weight, *nd* not detected

Significant differences according to Tukey's multiple comparison test ($a < 0.05$) are marked with different letters in the same row. All data are expressed as mean ± SD ($n \geq 3$)

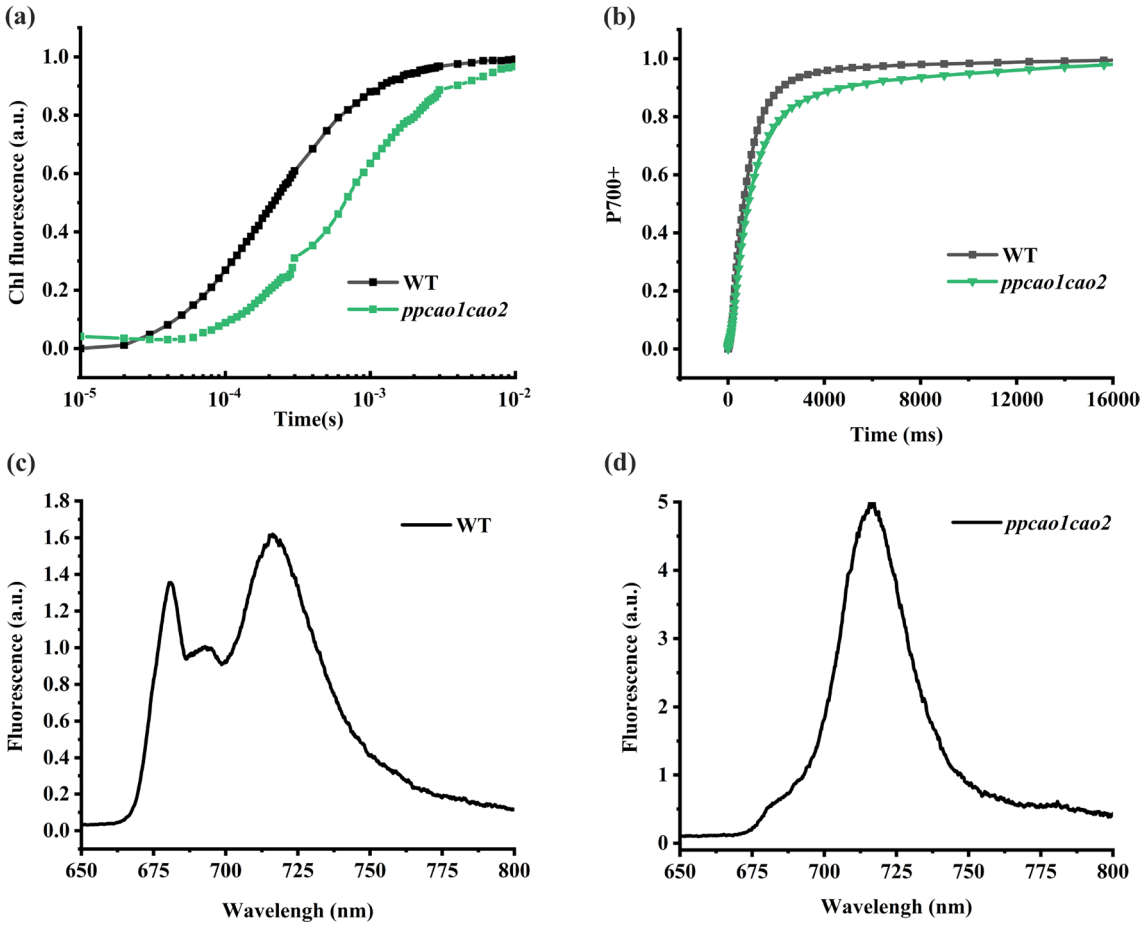

Fig. 2 Analysis of the functional antenna size of PS and the low temperature 77 K fluorescence emission spectra in *P. patens* WT and the *cao* double mutant. **a** Induction curves of Chl fluorescence in tissue of moss infiltrated with 20 μmol DCMU in dark for 40 min. **b** The kinetics of $P700^{+}$ formation in the presence of 30 μM DCMU and 100 μM methyl viologen (MV) in dark for 40 min. **c**, **d** The 77 K fluorescence emission spectra of *P. patens* WT and *ppcao1cao2* thylakoid membrane that were extracted in the growth light condition before rapidly freezing in liquid nitrogen. The spectra with excitation at 475 nm. All spectra were normalized at 693 nm. Data are expressed as mean ± SD ($n \geq 3$)

The low-temperature (77 K) fluorescence emission spectra of the *P. patens* WT thylakoid membranes had three characteristic peaks, located at 682, 693, and 717 nm, which were attributed to LHCII, PSII core, and PSI-LHCI, respectively, as previously reported (Pinnola et al. 2015). In *ppcao1cao2*, the peaks corresponding to LHCII and PSII core were significantly diminished, leaving only a prominent peak representing PSI (Fig. 2c, d).

Chl fluorescence and P700 redox analysis showed that *ppcao1cao2* had much lower PSII and PSI activities than WT (Fig. S8a, b). To investgated the kinetic of NPQ, we measured the time courses of NPQ of WT and *ppcao1cao2*

under actinic light of 50 and 830 µmol photons m^{-2} s^{-1} (Fig. S8d, Fig. 3). Under both circumstrances, NPQ was clearly induced in WT, but *ppcao1cao2* presented very low and plain NPQ kinetics. The *ppcao1cao2* presented a much higher Y(ND) and a similar level of Y(NA) compared with WT (Fig. S8c, e), suggesting that the reduction in Y(I) of *ppcao1cao2* can be attributed to limitations on the donor side.

The fluctuating light treatment (FL) simulates the unstable light conditions in the natural environment. All genotypes were exposed to FL consisting of a low-light phase (50 µmol photons m^{-2} s^{-1} for 5 min) and a high-light phase (500 µmol photons m^{-2} s^{-1} for 1 min) using the DUAL-PAM system. *ppcao1cao2* possessed quite lower Y(I) and Y(II) than WT since the first cycle (Fig. S9a, b). NPQ increased gradually with FL cycles in WT, but remained very low and insensitive to FL in *ppcao1cao2* (Fig. S9c). The reduction in Y(I) of *ppcao1cao2* was due to donor side limitation as indicated by high Y(ND) (Fig. S9d). The unchanged Fv/Fm and Pm of WT and *ppcao1cao2* before and after fluctuating light respectively indicated that the PSI and PSII were not photodamaged by the whole FL treatment in both genotypes (Fig. S9g, h).

The transcriptional level of genes related to photosynthesis

The expression levels of genes related to photosynthesis in WT and *ppcao1cao2* were determined by qRT-PCR. The results revealed that the transcription levels of *PsbB*, *PsbC*, *PsbD*, *PsaA*, *PsaO1*, *PsbS*, *LHCSR*, *FNR1*, *NdhA*, *PETE1*, *AtpA*, *PetA*, *PGR5* and *Flv* genes were upregulated in *ppcao1cao2*, whereas *PsbA*, *rbcL*, *Lhca1*, and *Lhcbm* were apparently downregulated in *ppcao1cao2* compared with those of the WT (Fig. 4).

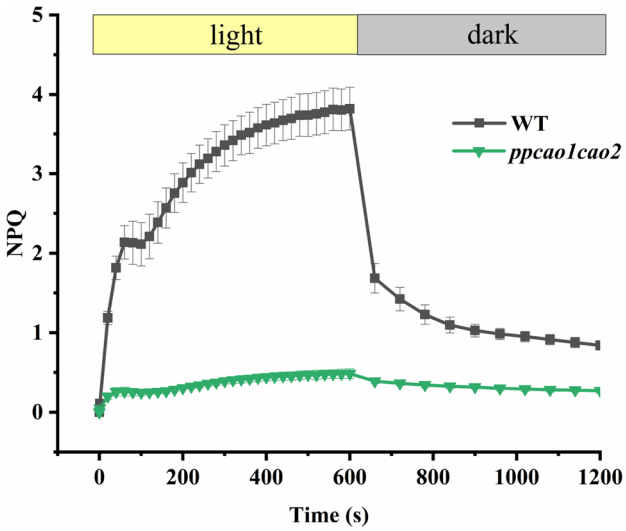

Fig. 3 NPQ characteristics of WT and *ppcao1cao2* mutant. Kinetics of NPQ induction and relaxation were recorded during a 10 min exposure to illumination at 830 µmol photons m^{-2} s^{-1} followed by 10 min recovery in darkness. Data are expressed as average ± SD ($n \geq 3$)

The accumulation of thylakoid membrane proteins in *ppcao1cao2*

We analyzed the thylakoid proteins composition by SDS-PAGE and immunodetection. We used antibodies for LHCB1, LHCB5 (LHCB6) and LHCA2 representing the major, the minor antenna of PSII and PSI antenna respectively for westernblotting and found that these antenna subunits were almost diminished in *ppcao1cao2* (Fig. 5). We also detected the subunits of other complexes on the thylakoid membranes. When thylakoid membrane samples with same amount of Chl *a* were loaded, more signals for bands representing PSII core subunits, PSI core subunits were observed in *ppcao1cao2*. LHCSR, an important NPQ player in *P. patens*, also accumulated more in *ppcao1cao2* than in WT (Fig. 5). There are no significant changes in the signals of Cty b_6f, ATPase and PsbS compared to WT (Fig. 5).

The organization and composition of the photosystems in *ppcao1cao2*

After solubilization in *β*-DM, the thylakoid membranes were separated by lpBN-PAGE to investigate composition of pigment protein complexes and the subunits comprising each protein complex were separated by 2D SDS-PAGE (Fig. 6). In *ppcao1cao2*, only three bands can be observed in lpBN-PAGE, representing PSI core complex, PSII core complex, and CP43-less PSII core complex, respectively (Fig. 6b). No bands representing PSII supercomplexes, PSII-LHC complex, LHCII trimer and LHCII monomers, which were present in WT, can be seen in *ppcao1cao2*. To investigate the distribution of PSII core proteins CP43 and CP47, western blotting after 2D SDS-PAGE were employed (Fig. 6c, d). The result showed that most CP47 were detected in the PSII core and CP43-less PSII core but only a small part of CP43 was found in the PSII core and a large amount of CP43 were detected as monomeric proteins in *ppcao1cao2* (Fig. 6d).

The P700 re-oxidation capacity of *ppcao1cao2*

The P700 re-oxidation phenomenon has been observed exclusively in non-flowering plants (Ilik et al. 2017). The P700 re-oxidation capacity was measured by exposure of dark-adapted samples to actinic light (2000 µmol photons m^{-2} s^{-1}). The initial oxidation of P700 (forming $P700^+$) reflects the intrinsic activity of PSI and the subsequent $P700^+$ reduction (forming P700) reflects the intake of

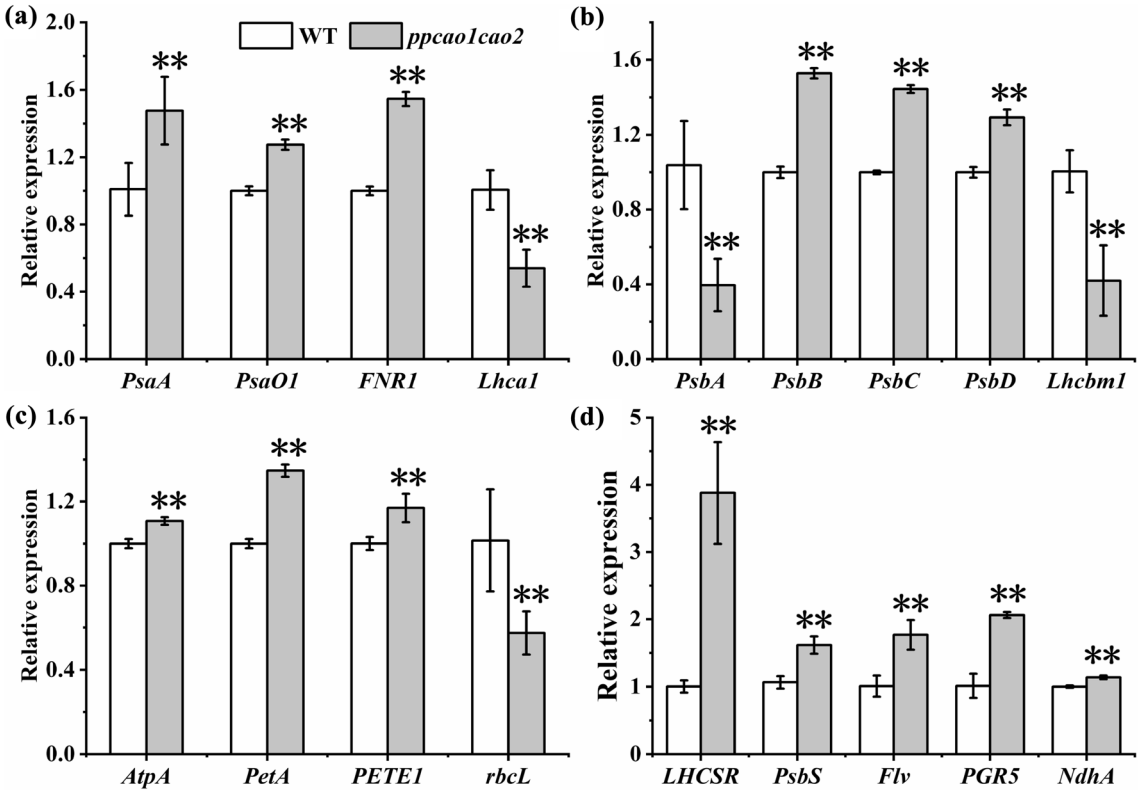

Fig. 4 Relative expression levels of the corresponding genes by qRT-PCR. CT values were calculated by *Actin1* expression levels, and error bars represent from the values obtained through three replications Data are expressed as mean ± SD ($n \geq 3$)

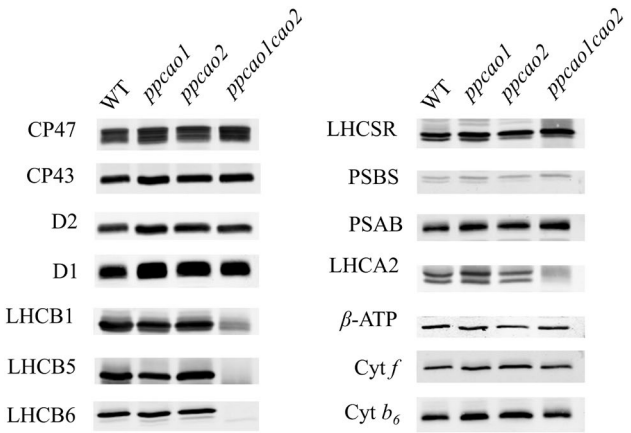

Fig. 5 Immunoblot analyses of thylakoid membranes of WT and *cao* mutants. The thylakoid membranes from all samples corresponding to 0.73 µg of Chl *a* were separated by SDS-PAGE for immunoblotting

electrons originating in water splitting at PSII, and the final re-oxidation of P700 can be attributed to the outflow of electrons from PSI (Schansker et al. 2003, 2005; Ilik et al. 2017). The result showed that after the initial oxidation of P700, WT presented a complete $P700^+$ reduction before subsequent re-oxidation. In *ppcao1cao2*, after the initial oxidation of P700, the extent of $P700^+$ reduction was much lower than in WT. notably, a faster re-oxidation rate was observed in *ppcao1cao2* than in WT when a 0-1normalization was employed (Fig. S10).

Discussion

The moss *P. patens*, with detailed genome information and easy transformation methods, has been developed as a model organism in bryophytes (Schaefer 2002). In the wild, Mosses might grow on both sunlight energy and organic chemicals from decomposed biomass under tree canopies where they frequently experience much higher irradiation than aquatic environments (Cove 2005; Way and Pearcy 2012; Iwai and Yokono 2017). Studies have shown that *P. patens* possesses more family members of genes encoding antenna proteins compared to its green algae and angiosperm counterparts, *Chlamydomonas* and *Arabidopsis* (Iwai and Yokono 2017). Furthermore, *P. patens* persists algal- and angiosperm-type qE pathway to quench excessive energy (Iwai and Yokono 2017) and besides cyclic electron transport (CEF), it possesses very active pseudo-cyclic electron transport (PCEF) to drive active electron to FLV proteins (Yamamoto et al. 2016; Ilik et al. 2017), which is lost in angiosperms.

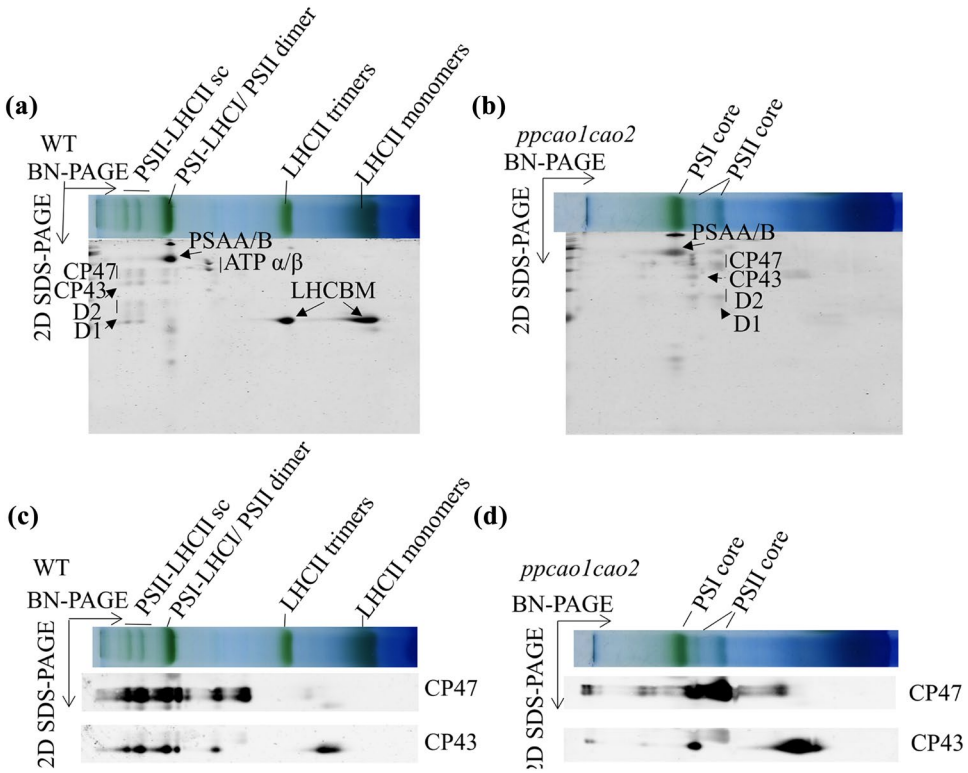

Fig. 6 2D-lpBN-SDS-PAGE of the thylakoid protein complexes in WT and *ppcao1cao2*. The thylakoid extracts of WT and *ppcao1cao2* were firstly separated by lpBN-PAGE. A total of 2.9 µg of Chl *a* was loaded in each lane. The strips of WT and *ppcao1cao2* were furtherly separated by 2D SDS-PAGE and stained with Coomassie brilliant blue G-250 (**a**, **b**) or immunoblotted with the antibodies for CP47 and CP43 (**c**, **d**)

In green plants, Chl *b* molecules are only found in LHCs and plays important roles in the folding and function of the LHC complexes (Green and Durnford 1996; Hoober et al. 2007). CAO is the key enzyme that catalyzes the conversion of Chl *a* to Chl *b*. The precise localization of CAO and its role in chloroplast protein import remain elusive, because CAO is present at extremely low levels in chloroplasts and is not detectable by immunological or mass spectrometry methods (Tanaka and Tanaka 2019). Our attempt to make antibodies for CAOs in *P. patens* also failed. All studied species of green plants have only one copy of *CAO* gene in their genomes except for rice, which has two tandem copies on one chromosome; however, only one copy is active and the other seems to be a pseudogene (Lee et al. 2005; Kunugi et al. 2013; Jung et al. 2021). In *P. patens*, two copies of *CAO* genes were found on different chromosomes. We found the transcription of two CAOs was differently regulated upon light exposure (Fig. 1). Using mutants deficient either or both *PpCAO*s achieved by CRISPR-Cas9 technology (Lopez-Obando et al. 2016), it was revealed that only when both *PpCAO*s were knock out did Chl *b* synthesis stop completely in *P. patens* (Table 1, Fig. S6). Therefore, unlike green algae or vascular plants, *P. patens* is equipped with two functional *CAO* genes to guarantee the Chl *b* synthesis.

Previous studies have shown that Chl *b* deficiency in green plants specifically impacts the accumulation of LHC apoproteins, while their mRNA levels remain unaffected (Espineda et al. 1999; Nick et al. 2013). Appropriate reduction of Chl *b* in *Chlamydomonas* and higher plants can improve the photosynthetic activity and biomass, but excessive reduction of Chl *b* will lead to decreased photosynthetic efficiency and light tolerance of plants (Mussgnug et al. 2007; Friedland et al. 2019; Wu et al. 2020). In our study, *ppcao1cao2*, due to Chl b deficiency, has a lower Fv/Fm (Fig. S7). The majority of chlorophyll fluorescence is emitted by PSII, excited by energy captured mostly by LHCII. When LHCII was eliminated in the mutant, the level of fluorescence was very low and the kinetics of fluorescence was steady. We found a lot of PSII core subunits such as CP43 exist in the monomeric form in vivo (Fig. 6), which would enhance the Fo level. We observed a significant decrease in the expression of *LHCBM* and *Lhca1*. However almost no antenna proteins accumulated in the thylakoid membranes which means the transcription of antenna protein genes were downregulated when Chl *b* synthesis was blocked and even there were some mRNAs of antenna proteins, very few antenna proteins were detected because the synthesis of antenna proteins and Chl *b* might be tightly correlated or the newly-synthesized antenna proteins were rapidly degraded when Chl *b* was unavailable. As for core complex subunits, we found that the expression of *PsbA* was decreased, but *PsbB*, *PsbC, PsbD* were increased (Fig. 4b), suggesting that the expression of D1 is regulated under a distinct pattern from that of the other PSII core subunits. The expression of *PsaA*, encoding one major PSI subunit was markedly increased (Fig. 4a), which is consistent with

findings in rice *cao* mutants (Jung et al. 2021). The expression of *PsaO* and *FNR1*, encoding two subunits of PSI, were also significantly increased (Fig. 4a). The final protein levels of both core complexes were similar in WT and *ppcao1cao2* on an equal Chl *a* amount basis (Fig. 5). This suggest that unlike antenna proteins, the expression of all detected core complexes subunit genes except *PsbA* in *ppcao1cao2* were enhanced (Fig. 4) and these subunit proteins can be synthesized and inserted into thylakoid membranes (Fig. 5), but a significant percentage of these proteins cannot be assembled into the whole complex and exist as monomeric form (Fig. 6). Moreover, genes encoding key players involved in NPQ, such as *PsbS* and *LHCSR*, as well as components related to CEF component *PGR5, NdhA* and PCEF component *Flv* were also enhanced in *ppcao1cao2* (Fig. 4c, d). Similarly, the expression of *PETE1* (encoding the major isoform of plastocyanin), *PetA* (encoding one cytochrome b_6f subunit), *AtpA* (encoding ATP synthase alpha subunit) were also increased (Fig. 4c). However, the protein levels of subunits from cytochrome b_6f and ATP synthase were not increased (Fig. 5), which means that post-transcriptional regulation might exist to repress the protein level of cytochrome b_6f and ATP synthase.

Previous studies on Chl *b*-less mutants of vascular plants or algae have shown that varying abilities of different LHCs to withstand Chl *b* deprivation. Generally speaking, LHCI is less sensitive to Chl *b* deprivation than LHCII. In vascular plants, the absence of Chl *b* reduces the levels of not only LHCII but also some other antenna proteins in chloroplasts to varying degrees (Tanaka and Tanaka 2005; Takabayashi et al. 2011). In *Chlamydomonas*, both LHCII and LHCI could accumulate to wild-type levels in a *CAO* mutant if Chl *a* synthesis remains unaltered (Bujaldon et al. 2017). However, in *ppcao1cao2*, the protein accumulation of antenna proteins for both photosystems was significantly reduced, as evidenced by SDS-PAGE and western blotting analysis (Figs. 5 and 6) and only PSI and PSII core complexes were observed in lpBN-PAGE (Fig. 6). LHCSR, an essential component in NPQ, does not bind Chl *b* for its correct folding and LHCSR was also found in diatoms, which lack Chl *b* (Koziol et al. 2007). The transcriptional expression and protein levels of LHCSR were enhanced in *ppcao1cao2* (Figs. 2d and 5). However, NPQ in *ppcao1cao2* still cannot develop (Figs. 3, S8d, S9c), likely due to the very low accumulation of LHCBM (Fig. 5). A similar result has been reported in the Chl *b*-less *Cbs3* strain of *Chlamydomonas*, where LHCSR3 accumulation failed to induce NPQ (Bonente et al. 2011). It had been shown that FLV-dependent PCEF, another fate of electrons past PSI, is especially active in fluctuating light conditions and essential for *P. patens* as safe valve (Gerotto et al. 2016; Ilik et al. 2017). In our results, although the $P700^+$ reduction was not complete in *ppcao1cao2* because of very low PSII activity (Fig. S10a), the kinetics of P700 re-oxidation was even faster than WT (Fig. S10b), partly resulting from higher expression of *Flv* (Fig. 4d). This pathway might consume active electrons at the acceptor side of PSI, decreasing Y(NA) (Figs. S8e, S9f), keeping PSI from damage by excessive electrons. This could explain why PSI core complexes were more stable than PSII complexes in *ppcao1cao2* (Fig. 6).

Conclusions

Both CAOs, PpCAO1 and PpCAO2, are needed to maintain the amount of Chl *b* in *P. patens*, in which the existence of Chl *b* and antenna proteins are tightly correlated. With almost no antenna complexes and NPQ, the *P. patens* Chl *b*-less mutant *ppcao1cao2* possesses much more functional PSI core complexes than PSII core complexes. The FLV-dependent PCEF activity in *ppcao1cao2* might be the major photoprotective process for PSI in the mutant.

Supplementary Information The online version contains supplementary material available at https://doi.org/10.1007/s11120-023-01044-8.

Author contributions CL and CY planned and designed the research. LZ and CL carried out the experiments and took part in the data analysis. LZ and CL wrote the manuscript.

Funding This work was supported by the Academician Workstation of Agricultural High-tech Industrial Area of the Yellow River Delta, National Center of Technology Innovation for Comprehensive Utilization of Saline-Alkali Land, Dongying, Shandong, China and Science & Technology Specific Projects in Agricultural High-tech Industrial Demonstration Area of the Yellow River Delta (Grant No: 2022SZX12) and the National Key R&D Program of China (Grant No: 2017YFA0503701).

Data availability It is not applicable.

Declarations

Conflict of interest The authors declare no conflicts of interest.

References

Ashton NW, Grimsley NH, Cove DJ (1979) Analysis of gametophytic development in the moss, *Physcomitrella patens*, using auxin and cytokinin resistant mutants. Planta 144:427–435. https://doi.org/10.1007/bf00380118

Bonente G, Ballottari M, Truong TB et al (2011) Analysis of LhcSR3, a protein essential for feedback de-excitation in the green alga *Chlamydomonas reinhardtii*. PLoS Biol 9:e1000577. https://doi.org/10.1371/journal.pbio.1000577

Bujaldon S, Kodama N, Rappaport F et al (2017) Functional accumulation of antenna proteins in chlorophyll *b*-Less Mutants of *Chlamydomonas reinhardtii*. Mol Plant 10:115–130. https://doi.org/10.1016/j.molp.2016.10.001

Casazza AP, Tarantino D, Soave C (2001) Preparation and functional characterization of thylakoids from *Arabidopsis thaliana*. Photosynth Res 68:175–180. https://doi.org/10.1023/a:1011818021875

Cove D (2005) The Moss *Physcomitrella patens*. Annu Rev Genet 39:339–358. https://doi.org/10.1146/annurev.genet.39.073003.110214

Dall'Osto L, Cazzaniga S, Havaux M et al (2010) Enhanced photoprotection by protein-bound vs free xanthophyll pools: a comparative analysis of chlorophyll *b* and xanthophyll biosynthesis mutants. Mol Plant 3:576–593. https://doi.org/10.1093/mp/ssp117

Derks A, Schaven K, Bruce D (2015) Diverse mechanisms for photoprotection in photosynthesis: dynamic regulation of photosystem II excitation in response to rapid environmental change. Biochem Biophys Acta 1847:468–485. https://doi.org/10.1016/j.bbabio.2015.02.008

Eggink LL, LoBrutto R, Brune DC et al (2004) Synthesis of chlorophyll *b*: localization of chlorophyllide a oxygenase and discovery of a stable radical in the catalytic subunit. BMC Plant Biol 4:5. https://doi.org/10.1186/1471-2229-4-5

Espineda CE, Linford AS, Devine D et al (1999) The AtCAO gene, encoding chlorophyll a oxygenase, is required for chlorophyll b synthesis in *Arabidopsis thaliana*. PNAS 96:10507–10511. https://doi.org/10.1073/pnas.96.18.10507

Friedland N, Negi S, Vinogradova-Shah T et al (2019) Fine-tuning the photosynthetic light harvesting apparatus for improved photosynthetic efficiency and biomass yield. Sci Rep 9:13028. https://doi.org/10.1038/s41598-019-49545-8

Gerotto C, Alboresi A, Giacometti GM et al (2012) Coexistence of plant and algal energy dissipation mechanisms in the moss *Physcomitrella patens*. New Phytol 196:763–773. https://doi.org/10.1111/j.1469-8137.2012.04345.x

Gerotto C, Alboresi A, Meneghesso A et al (2016) Flavodiiron proteins act as safety valve for electrons in *Physcomitrella patens*. PNAS 113:12322–12327. https://doi.org/10.1073/pnas.1606685113

Gerotto C, Trotta A, Bajwa AA et al (2019) Thylakoid protein phosphorylation dynamics in amoss mutant lacking serine/threonine protein kinase STN8. Plant Physiol 180:1582–1597. https://doi.org/10.1104/pp.19.00117

Giovagnetti V, Ruban AV (2018) The evolution of the photoprotective antenna proteins in oxygenic photosynthetic eukaryotes. Biochem Soc Trans 46:1263–1277. https://doi.org/10.1042/bst20170304

Green BR, Durnford DG (1996) The chlorophyll-carotenoid proteins of oxygenic photosynthesis. Annu Rev Plant Physiol Plant Mol Biol 47:685–714. https://doi.org/10.1146/annurev.arplant.47.1.685

Greene BA, Staehelin LA, Melis A (1988) Compensatory alterations in the photochemical apparatus of a photoregulatory, chlorophyll *b*-deficient mutant of Maize. Plant Physiol 87:365–370. https://doi.org/10.1104/pp.87.2.365

Havaux M, Dall'osto L, Bassi R (2007) Zeaxanthin has enhanced antioxidant capacity with respect to all other xanthophylls in *Arabidopsis* leaves and functions independent of binding to PSII antennae. Plant Physiol 145:1506–1520. https://doi.org/10.1104/pp.107.108480

Hoober JK, Eggink LL, Chen M (2007) Chlorophylls, ligands and assembly of light-harvesting complexes in chloroplasts. Photosynth Res 94:387–400. https://doi.org/10.1007/s11120-007-9181-1

Horn R, Grundmann G, Paulsen H (2007) Consecutive binding of chlorophylls *a* and *b* during the assembly in vitro of light-harvesting chlorophyll-*a*/*b* protein (LHCIIb). J Mol Biol 366:1045–1054. https://doi.org/10.1016/j.jmb.2006.11.069

Ilik P, Pavlovic A, Kouril R et al (2017) Alternative electron transport mediated by flavodiiron proteins is operational in organisms from cyanobacteria up to gymnosperms. New Phytol 214:967–972. https://doi.org/10.1111/nph.14536

Iwai M, Yokono M (2017) Light-harvesting antenna complexes in the moss *Physcomitrella patens*: implications for the evolutionary transition from green algae to land plants. Curr Opin Plant Biol 37:94–101. https://doi.org/10.1016/j.pbi.2017.04.002

Iwai M, Yokono M, Kono M et al (2015) Light-harvesting complex Lhcb9 confers a green alga-type photosystem I supercomplex to the moss *Physcomitrella patens*. Nature Plants 1:14008. https://doi.org/10.1038/nplants.2014.8

Järvi S, Suorsa M, Paakkarinen V et al (2011) Optimized native gel systems for separation of thylakoid protein complexes: novel super- and mega-complexes. Biochemical Journal 439:207–214. https://doi.org/10.1042/BJ20102155

Jung YJ, Lee HJ, Yu J et al (2021) Transcriptomic and physiological analysis of *OsCAO1* knockout lines using the CRISPR/Cas9 system in rice. Plant Cell Rep 40:1013–1024. https://doi.org/10.1007/s00299-020-02607-y

Kim EH, Li XP, Razeghifard R et al (2009) The multiple roles of light-harvesting chlorophyll *a*/*b*-protein complexes define structure and optimize function of *Arabidopsis* chloroplasts: a study using two chlorophyll *b*-less mutants. Biochem Biophys Acta 1787:973–984. https://doi.org/10.1016/j.bbabio.2009.04.009

Koziol AG, Borza T, Ishida K et al (2007) Tracing the evolution of the light-harvesting antennae in chlorophyll a/b-containing organisms. Plant Physiol 143:1802–1816. https://doi.org/10.1104/pp.106.092536

Kunugi M, Takabayashi A, Tanaka A (2013) Evolutionary changes in chlorophyllide a oxygenase (CAO) structure contribute to the acquisition of a new light-harvesting complex in micromonas. J Biol Chem 288:19330–19341. https://doi.org/10.1074/jbc.M113.462663

Lee S, Kim JH, Yoo ES et al (2005) Differential regulation of chlorophyll a oxygenase genes in rice. Plant Mol Biol 57:805–818. https://doi.org/10.1007/s11103-005-2066-9

Lopez-Obando M, Hoffmann B, Géry C et al (2016) Simple and efficient targeting of multiple genes through CRISPR-Cas9 in *Physcomitrella patens*. G3-Genes Genom Genet 6:3647–3653. https://doi.org/10.1534/g3.116.033266

Malkin S, Armond PA, Mooney HA et al (1981) Photosystem II photosynthetic unit sizes from fluorescenceinduction in leaves. Plant Physiol 67:570–579. https://doi.org/10.1104/pp.67.3.570

Müller P, Li XP, Niyogi KK (2001) Non-photochemical quenching: a response to excess light energy. Plant Physiol 125:1558–1566. https://doi.org/10.1104/pp.125.4.1558

Mussgnug JH, Thomas-Hall S, Rupprecht J et al (2007) Engineering photosynthetic light capture: impacts on improved solar energy to biomass conversion. Plant Biotechnol J 5:802–814. https://doi.org/10.1111/j.1467-7652.2007.00285.x

Nagata N, Satoh S, Tanaka R et al (2004) Domain structures of chlorophyllide a oxygenase of green plants and *Prochlorothrix hollandica* in relation to catalytic functions. Planta 218:1019–1025. https://doi.org/10.1007/s00425-003-1181-6

Nick S, Meurer J, Soll J et al (2013) Nucleus-encoded light-harvesting chlorophyll *a*/*b* proteins are imported normally into chlorophyll *b*-free chloroplasts of *Arabidopsis*. Mol Plant 6:860–871. https://doi.org/10.1093/mp/sss113

Oster U, Tanaka R, Tanaka A et al (2000) Cloning and functional expression of the gene encoding the key enzyme for chlorophyll *b* biosynthesis (*CAO*) from *Arabidopsis thaliana*. Plant J 21:305–310. https://doi.org/10.1046/j.1365-313x.2000.00672.x

Perrine Z, Negi S, Sayre RT (2012) Optimization of photosynthetic light energy utilization by microalgae. Algal Res 1:134–142. https://doi.org/10.1016/j.algal.2012.07.002

Pinnola A, Dall'Osto L, Gerotto C et al (2013) Zeaxanthin binds to light-harvesting complex stress-related protein to enhance nonphotochemical quenching in *Physcomitrella patens*. Plant Cell 25:3519–3534. https://doi.org/10.1105/tpc.113.114538

Pinnola A, Cazzaniga S, Alboresi A et al (2015) Light-harvesting complex stress-related proteins catalyze excess energy dissipation in both photosystems of *Physcomitrella patens*. Plant Cell 27:3213–3227. https://doi.org/10.1105/tpc.15.00443

Pinnola A, Alboresi A, Nosek L et al (2018) A LHCB9-dependent photosystem I megacomplex induced under low light in *Physcomitrella patens*. Nat Plants 4:910–919. https://doi.org/10.1038/s41477-018-0270-2

Qin XC, Suga M, Kuang T et al (2015) Structural basis for energy transfer pathways in the plant PSI-LHCI supercomplex. Science 348:989–995. https://doi.org/10.1126/science.aab0214

Rensing SA, Lang D, Zimmer AD et al (2008) The *Physcomitrella* genome reveals evolutionary insights into the conquest of land by plants. Science 319:64–69. https://doi.org/10.1126/science.1150646

Schaefer DG (2002) A new moss genetics: targeted mutagenesis in *Physcomitrella patens*. Annu Rev Plant Biol 53:477–501. https://doi.org/10.1146/annurev.arplant.53.100301.135202

Schaefer DG, Zrÿd JP (1997) Efficient gene targeting in the moss *Physcomitrella patens*. Plant J 11:1195–1206. https://doi.org/10.1046/j.1365-313x.1997.11061195.x

Schansker G, Srivastava A, Strasser RJ (2003) Characterization of the 820-nm transmission signal paralleling the chlorophyll *a* fluorescence rise (OJIP) in pea leaves. Funct Plant Biol 30:785–796. https://doi.org/10.1071/fp03032

Schansker G, Tóth SZ, Strasser RJ (2005) Methylviologen and dibromothymoquinone treatments of pea leaves reveal the role of photosystem I in the Chl *a* fluorescence rise OJIP. Biochim Biophys Acta 1706:250–261. https://doi.org/10.1016/j.bbabio.2004.11.006

Takabayashi A, Kurihara K, Kuwano M et al (2011) The oligomeric states of the photosystems and the light-harvesting complexes in the Chl *b*-less mutant. Plant Cell Physiol 52:2103–2114. https://doi.org/10.1093/pcp/pcr138

Tanaka R, Tanaka A (2005) Effects of chlorophyllide *a* oxygenase overexpression on light acclimation in *Arabidopsis thaliana*. Photosynth Res 85:327–340. https://doi.org/10.1007/s11120-005-6807-z

Tanaka R, Tanaka A (2011) Chlorophyll cycle regulates the construction and destruction of the light-harvesting complexes. Biochem Biophys Acta 1807:968–976. https://doi.org/10.1016/j.bbabio.2011.01.002

Tanaka A, Tanaka R (2019) The biochemistry, physiology, and evolution of the chlorophyll cycle—ScienceDirect. Adv Bot Res 90:183–212. https://doi.org/10.1016/bs.abr.2019.03.005

Tanaka A, Ito H, Tanaka R et al (1998) Chlorophyll *a* oxygenase (CAO) is involved in chlorophyll *b* formation from chlorophyll *a*. PNAS 95:12719–12723. https://doi.org/10.1073/pnas.95.21.12719

Thayer SS, Björkman O (1990) Leaf xanthophyll content and composition in sun and shade determined by HPLC. Photosynth Res 23:331–343. https://doi.org/10.1007/BF00034864

Way DA, Pearcy RW (2012) Sunflecks in trees and forests: from photosynthetic physiology to global change biology. Tree Physiol 32:1066–1081. https://doi.org/10.1093/treephys/tps064

Wu G, Ma L, Sayre RT et al (2020) Identification of the optimal light harvesting antenna size for high-light stress mitigation in plants. Front Plant Sci 11:505. https://doi.org/10.3389/fpls.2020.00505

Yamamoto H, Takahashi S, Badger MR et al (2016) Artificial remodelling of alternative electron flow by flavodiiron proteins in *Arabidopsis*. Nat Plants 2:16012. https://doi.org/10.1038/nplants.2016.12

Yan Q, Zhao L, Wang W et al (2021) Antenna arrangement and energy-transfer pathways of PSI-LHCI from the moss *Physcomitrella patens*. Cell Discov 7:10. https://doi.org/10.1038/s41421-021-00242-9

Yang C, Kosemund K, Cornet C et al (1999) Exchange of pigment-binding amino acids in light-harvesting chlorophyll *a*/*b* protein. Biochemistry 38:16205–16213. https://doi.org/10.1021/bi990738x